

Automated Detection of Clouds in Satellite Imagery

Gary Jedlovec
NASA Marshall Space Flight Center
USA

1. Introduction

The detection of clouds in satellite imagery has a number of important applications in weather and climate studies. The presence of clouds can alter the energy budget of the Earth-atmosphere system through scattering and absorption of shortwave radiation and the absorption and re-emission of infrared radiation at longer wavelengths. The scattering and absorption characteristics of clouds vary with the microphysical properties of clouds, hence the cloud type. Thus, detecting the presence of clouds over a region in satellite imagery is important in order to derive atmospheric or surface parameters (e.g., optical depth, phase, temperature, etc.) that give insight into weather and climate processes. For many applications however, clouds are a contaminant whose presence interferes with retrieving atmosphere or surface information. In these cases, the detection of cloud contaminated pixels in satellite imagery is important to isolate cloud-free pixels used to retrieve atmospheric thermodynamic information (e.g., temperature and moisture information, ozone content, and even trace gas concentrations) or surface geophysical parameters (e.g., land and sea surface temperature, vegetation information, etc.) from cloudy ones.

The ability to derive an accurate cloud mask from geostationary and polar orbiting satellite data under a variety of conditions has been a research topic since the launch of the first Earth observing satellite TIROS-1 in 1960. The limited success of some early studies (Coakley and Bretherton 1982; Rossow and Garder 1993; and those discussed by Goodman and Sellers 1988) suggests that the accurate detection of clouds in satellite imagery both during the day and at night is a challenging problem. In more recent work, the probability of detecting clouds has been reported to exceed 90% (Saunders and Kriebel 1988; Merchant et al. 2005; Jedlovec et al. 2008; Reuter et al. 2009) but the performance varies seasonally, regionally, with time of day and retrieval technique. While traditionally both spatial and spectral techniques have been employed to identify cloud contaminated pixels in polar orbiting and geostationary satellite data, sensor spatial resolution, the lack of surface – atmospheric boundary layer temperature contrast, and surface emissivity variations all present performance challenges to a given cloud detection approach. Thus, any one technique may not be best suited for all applications, but may perform quite well in a particular environment (usually the environment in which the algorithm was developed and tested). *The key to the success of most of these algorithms lies in the selection of the*

thresholds for various spectral tests. In more robust algorithms, spatially and temporally varying thresholds, which better capture local atmospheric and surface effects, are used to improve their performance and broaden their application over algorithms with fixed thresholds for cloud tests.

In this chapter, a review of several multispectral cloud detection techniques is presented. Emphasis is placed on techniques which use multispectral approaches applicable to a wide variety of current and future satellite sensors. The detailed methodology used in several recent and widely used algorithms is highlighted. The performance of two cloud detection approaches is compared for the same observational conditions.

2. Theoretical approaches

Clouds have a high solar reflectivity at visible wavelengths compared to that of most surface features as shown in Figure 1. Spatial differentiation and thresholding techniques can be used with Earth viewing satellites measuring reflected solar energy to distinguish clouds from less reflective land and ocean surfaces. These methods are applicable during the day when solar illumination angles are sufficiently large and the reflected sunlight provides contrast in image features.

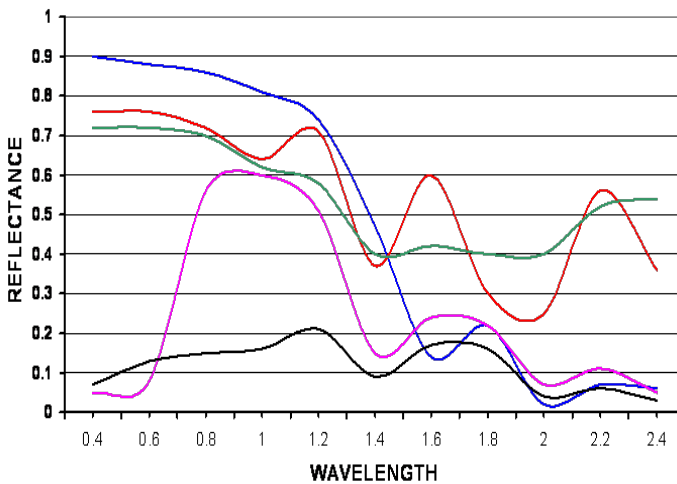


Fig. 1. Typical reflectance values for snow (blue), bare soil (black), forest canopy (pink), and cirrus (red) and stratus (green) clouds as a function of wavelength (micrometers).

Automated detection methods which use spatial analysis techniques to detect the contrast between reflected energy from clouds and surrounding (less reflective) scenes can be used to determine the extent of cloud cover over a region. This approach has difficulties under low solar illumination conditions and when other highly reflective non-cloud surfaces are present (e.g., snow, ice, sand) or other complicating optical conditions exist (e.g., scattering due to aerosols). Predetermined energy threshold values based on solar illumination angles can be used to delineate cloudy from cloud-free pixels in satellite imagery as well. This approach provides higher resolution cloud information (down to the pixel level) but is

heavily dependent on the determination of the threshold values. Appropriate threshold values usually change temporally, seasonally, and spatially, making the use of a fixed set of values limiting. The use of multiple channels in the visible (0.4-0.7 micrometers) and near or reflective infrared portion of the energy spectrum (0.7 – 2.5 micrometers), can help in the detection of clouds. Figure 2 presents an example of how reflectance information from satellite imagery can be used in a compositing technique to differentiate clouds from snow on the ground. The image on the left is a natural color composite which uses information from three channels in the visible region of the solar spectrum to replicate what the human eye would see from space. From the reflectance signatures in Figure 1, one would expect that snow and clouds would look similar at the visible wavelengths (and in fact this is the case for the natural color composite). The image on the right is a false color composite which uses one visible channel and two reflective infrared channels at 1.6 and 2.2 micrometers to differentiate clouds (white) from snow on the ground (red). Snow has a much lower reflectance value at the longer wavelengths as indicated in Figure 1. The use of multispectral measurements from satellite sensors can add significant skill in the detection of clouds from space.

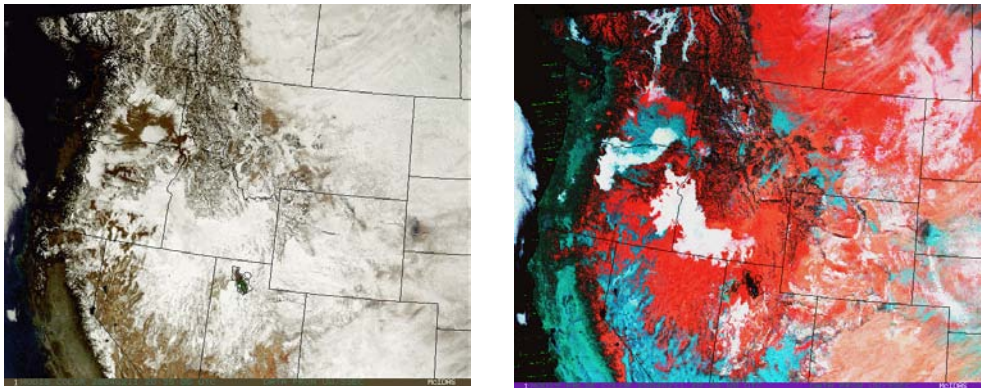


Fig 2. Multispectral natural (left) and false (right) color composite images derived from MODIS data on February 11, 2004 at 2035 UTC over the northwest portion of the United States. The false color composite uses near infrared channels to delineate clouds (white) from snow on the ground (red).

Clouds also emit thermal energy proportional to the product of their emissivity and temperature. Clouds generally take on their ambient environment temperature which, under normal lapse rate conditions, decreases with height in the atmosphere. Therefore when emission is converted to equivalent blackbody temperature it can be used to distinguish the presence opaque clouds from a warm surface with various thresholding techniques. Thermal imagery (as measured from satellites in the 8.0-12.0 micrometer window region) usually provides only limited contrast between cloudy and clear regions however, allowing for the detection of only high (cold) clouds with single channel techniques. Most cloud detection approaches use thermal emission variations at short (3.5-4.0 micrometers) and long thermal wavelengths (10.0-12.0 micrometers) to differentiate clouds from cloud-free scenes based on spectral difference thresholds. As with the visible

and near infrared spectral tests, emission and reflectance characteristics of the surface and clouds vary considerable with time, season, and region, limiting the use of fixed thresholds for successful cloud detection. The successful use of infrared detection methods relies on the determination of appropriate test thresholds.

An underlying principle applied with spectral difference tests using longwave and shortwave infrared window channels is that the difference between the emissivity of clouds at these wavelengths (e.g., 11.0 and 3.9 micrometers) varies from that for the surface (land or ocean). This difference can be inferred from channel brightness temperature differences and used to detect various types of clouds. The spectral emissivity varies at both of these wavelengths and with surface and cloud type, with the emissivity at the shortwave infrared wavelengths being smaller than at the longwave infrared wavelengths, resulting in lower emission temperatures at the shorter wavelengths. However, during the day reflected solar radiation (in the 3.0-4.0 micrometer region) makes the effective brightness temperatures (sum of emission and reflective components) at the shorter wavelengths larger than the brightness temperatures at the longer wavelengths even though the emissivity is less. For cloudy pixels, the longwave minus shortwave brightness temperature difference has a large negative value during the day, and at night a positive value for opaque clouds (thick water clouds and fog) because of the absence of solar radiation, and a negative value for thin ice clouds. Even though the emissivity of thin ice clouds is greater at long wavelengths than at short wavelengths, much of the energy sensed by the satellite comes from the Earth's surface and atmosphere below the cloud and the 3.9 micrometer channel's response to warm sub-pixel temperatures is greater than it is at 11.0 micrometer, resulting in negative difference values both during the day and during the night. Because the difference between shortwave and longwave emissivities is on average smaller for land and water than for clouds, cloud-free pixels will have a small negative temperature difference value during the day and a small negative or positive value at night.

The spectral properties of clouds and the Earth's surface allow for the delineation of clear and cloudy regions in thermal image as a discontinuity in the longwave minus shortwave brightness temperature difference image. Emissivity variation with cloud type affects the reflected component of the shortwave channel (due to varying solar input at the surface or cloud top) and makes the use of these channel differences for cloud detection a useful but challenging option in cloud detection. Figure 3 shows an example of a nighttime 11.0 - 3.9 micrometer difference image (top) and the corresponding infrared image (bottom) from the GOES satellite operated by NOAA. Notice that the warmer water clouds such as those over Texas and over the Atlantic Ocean, indicated by mid-to-light gray in the infrared image, have positive difference image values (indicated by yellow in the difference image). The colder thinner clouds shown as very light gray to white in the infrared image such as seen over New Mexico, Colorado and Iowa, have negative values (aqua colored clouds in the difference image). The clear land and water pixels have small negative or positive values, and are shown in gray shades in the difference image.

Figure 3 also highlights some of the complexities of using the difference imagery. Notice how in the infrared image the clouds over Kentucky and Tennessee appear to be of similar temperature as those over Arkansas and Louisiana, but the majority of the clouds in the former group have positive difference image values compared to the latter group having negative values. However, there are clouds that are easily seen in the infrared image, such as the large cloud feature over Louisiana, that are not indicated as clouds in the difference

image, but have difference values similar to the surface. The key to the successful detection of clouds with these properties lies in the selection of an appropriate threshold value for the 11 - 3.9 micrometer difference image test which separates cloud-free pixels (where the sensor observes the land) from cloudy pixels. The use of a fixed threshold will not produce good results in this situation.

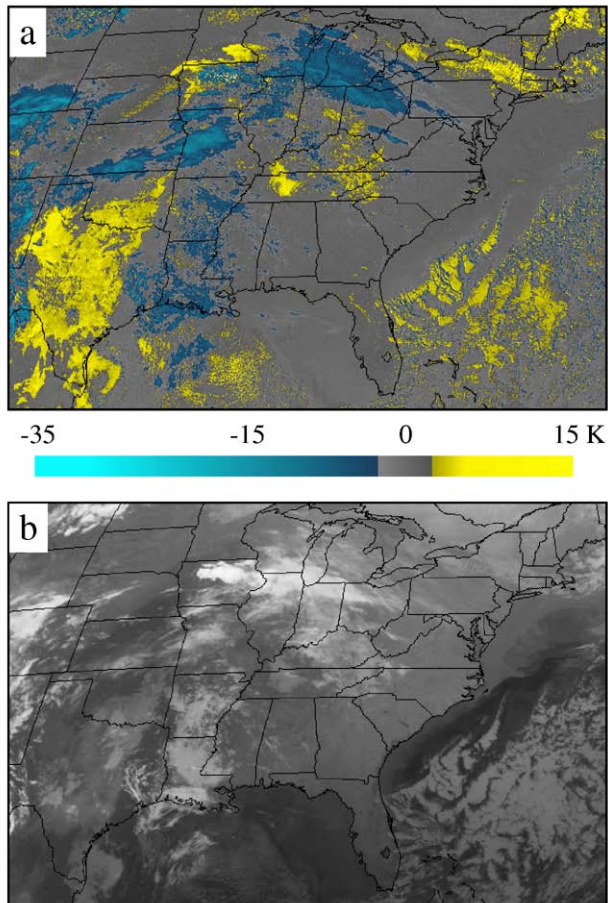


Fig. 3. Typical GOES nighttime 11.0-3.9 micrometer difference image (top) and 11.0 micrometer image (bottom) over the eastern two-thirds of the U.S.

2.1 Traditional approaches

Numerous approaches for the automatic detection of clouds have been applied to visible and infrared data from geostationary and polar-orbiting satellites. Some of these approaches considered the spatial variance of infrared radiances within a region to separate the points into clear or cloudy scenes (Coakley and Bretherton, 1982). The International Satellite Cloud Climatology Project (ISCCP) used visible and infrared data that included a series of both

spatial and temporal tests (Rossow and Garder, 1993). Other researchers such as Simpson and Gobat (1995a) presented a clustering algorithm for GOES data over land and an adaptive thresholding algorithm over ocean (Simpson and Gobat, 1995b), both for daytime scenes.

2.2 Advanced and operational techniques

An approach used operationally by the NOAA National Environmental Satellite, Data and Information Service (NESDIS) for the detection of clouds in GOES Imager and Sounder data for atmospheric applications is discussed by Schreiner et al. (2001) and Schreiner (2001). Their approach derived cloud information using a limited number of visible and infrared channels both during the day and at night. The scheme delineates between cloud-free pixels used for atmospheric product retrievals and cloudy pixels which are used to derive cloud parameters such as cloud top pressure, temperature, effective cloud amount, and other atmospheric products. The NESDIS approach uses four infrared window channels (the 12.7, 12.1, 11.0 and 3.9 μm channels) and the 13.4 micrometer carbon dioxide channel on GOES in the determination of sky conditions. The approach is broken up into a series of channel tests; the first two applied to a 3 x 3 array of pixels, and the last one applied to individual pixels. The first set of tests uses a simple 11.0 micrometer threshold test (with a cloud threshold derived from an estimated surface temperature minus 20 K), a visible channel reflectance test (with a background cloud-free albedo threshold value of 25% over land and 7% over water), and a nighttime inversion test (based on the shortwave and longwave infrared channel difference). A second set of tests includes a cold sea test, skin temperature retrieval test, and a reflected sunlight test (based on the infrared channel difference compared to a 25 K threshold value). The final set of tests is applied to each individual field of view and includes tests for snow (visible reflectance), stratus (11.0 -12.0 micrometer against a fixed threshold value based on channel noise), and thin cirrus (based on 13.4 micrometer band comparison to an assumed "cloud-free" value). This method is both complex in its application and requires the use of a number of different threshold values in the channel tests.

Another popular cloud detection technique was developed to detect clouds in AVHRR data on the NOAA polar orbiting satellites (Saunders and Kriebel 1988). The method uses data from visible and infrared channels on the AVHRR instrument in several cloud threshold tests to determine if pixels are cloudy or cloud-free. The first test is an infrared threshold test which compares the 11.0 micrometer channel brightness temperature to an estimate of SST or land surface temperature. The test is applied day and night and thresholds are determined by computing weekly averages of SSTs, and subjectively determined thresholds over land based on observed data. The second test is a spatial coherence test which evaluates the standard deviation of brightness temperatures in a 3 x 3 array of 11.0 micrometer pixels (Coakley and Bretherton 1982). The test is applied over the ocean during the day and land and ocean at night. The presence of clouds in a 3 x 3 pixel region will cause the standard deviation to exceed background scene variations. The third test is a dynamic reflectance test which is applied during the day. Histograms of visible reflectances (over land) and near infrared reflectances (over water) for a 50 x 50 pixel region are used to determine thresholds which isolate pixel values corresponding to clouds. An additional test involved evaluating the ratio of the near infrared to the visible channel reflectances during the day. Values close to unity indicate cloudy pixels. Assigned thresholds above and below 1.0 are used to determine cloud-free pixels. A fifth test evaluates a group of split window

channel differences between the 11.0-3.7, 3.7-12.0, and 11.0-12.0 micrometer split window channel difference for each pixel.

The oceans group at NESDIS have also applied a probability-based cloud detection approach to mask clouds in the generation of a global sea surface temperature product from GOES and AVHRR data (Maturi et al. 2008). This approach is an adaptation of the Bayesian method of Merchant et al. (2005) in which an estimate of the probability of clear sky is made for each pixel in the night-time imagery. This approach uses observational texture elements consisting of the standard deviation of the 3.7 and 11.0 micrometer brightness temperatures over a 3×3 pixel box as the observation vectors. The background state vector which describes the prior knowledge of the atmosphere and surface thermodynamic state is taken from forward radiative transfer calculations using numerical model forecasts relevant to the observational environment. The joint probability function for cloudy pixels is obtained from past 3.7 and 11.0 micrometer imagery. This approach brings in the window brightness temperature differences used in other approaches. By choosing a probability threshold, the Bayesian method allows one to generate a binary mask which provides optimal performance for a given application.

The National Aeronautics and Space Administration (NASA) EOS science team has developed an elaborate cloud detection technique for MODIS data on the Terra and Aqua polar orbiting satellites. The approach uses a series of threshold tests applied to many of the 36 MODIS channels to identify clouds in individual pixels (Ackerman et al. 1998; King et al. 2003). Test thresholds are used for various surface types and at different times of the day. Each cloud detection test returns a confidence level (1.0 for high confidence and 0.0 for low confidence) that the pixel is clear. Tests which are capable of detecting similar cloud conditions are grouped together and a minimum confidence is determined for each group. The final cloud mask is then determined from the product of the results from individual groups. The algorithm uses 10 spectral tests with varying threshold values based upon the underlying scene. These tests include single channel threshold tests with the 11.0, 13.9, and 6.7 micrometer channels with nominal threshold values of 270, 224, and 220 K respectively. These tests determine the presence of opaque cold clouds quite well. The algorithm also uses a test of the 11.0 micrometer window channel against the surface temperature for warm cloud detection. Four channel difference tests are also used in the technique. The 11.0 - 12.0 micrometer test is the traditional split window test used with AVHRR data. The 11.0 - 3.9 micrometer channel is effective in detecting clouds at night because of emissivity variations. The 3.9 - 12.0 micrometer and 7.2 - 11.0 micrometer tests are useful at high latitudes with the appropriate test thresholds. The 8.6 - 7.2 micrometer channel difference is also used at night in polar regions. A series of tri-spectral tests with the 8.6, 11.0, and 12.0 micrometer channels account for variations in ice and water absorption under varying water vapor conditions. A group of visible and near infrared reflectance tests are also used during the day. These involve single channel reflectance tests at 0.66, 0.86, and 1.38 micrometers, and ratios of the 0.86 / 0.66 micrometer channels. In all cases a range of values around a scene dependent threshold is used to bound the confidence in the test.

The bispectral composite threshold (BCT) method (Jedlovec et al. 2008) uses multispectral channel differences to contrast clear and cloudy regions in satellite imagery. The BCT method uses the 11.0 and 3.9 micrometer spectral channels in a four-step cloud detection procedure, comprising of two spatial tests and two spectral tests. The two spatial tests and one of the spectral tests are applied to the 11.0 and 3.9 micrometer difference imagery, and

the second spectral test is applied to the 11.0 micrometer image. The first test subjects each pixel in the 11.0 - 3.9 micrometer brightness temperature difference image to an adjacent pixel test. The variance between adjacent pixels along the scan line in the difference image is compared to a threshold value to detect a cloud edge. The threshold value is fixed for all pixels at 7.0 K and was subjectively determined from viewing a large number of difference image fields. This test is most successful in identifying the edges of clouds during the day. The second step in the BCT method attempts to fill-in between the cloud edges by analyzing the one-dimensional spatial variability of the pixels. The difference between two adjacent pixels is calculated. For a cloud to be detected, this calculated difference value must be less than the cloudy threshold value if the preceding image location was cloudy, or it must be either less than the negative of the clear threshold value or greater than two-thirds of the clear threshold if the preceding image location was clear. In this way the spatial variability in the difference image corresponding to a cloud free surface versus a cloud is considered. Threshold values of 3.0 and 0.0 K, for the clear and cloudy regions, respectively, were derived in a similar fashion as for the first spatial test. The threshold values for these first two tests can be adjusted (tuned) to tweak algorithm performance for particular applications and regions. These tests only detect a small percentage of clouds. However, these clouds are usually on the edge of a larger cloud field, and are diffuse or only partially contaminate a pixel in the image, and are not easily detected by other means.

The third step in the BCT method is used to detect clouds in regions where the first two steps do not detect clouds. It utilizes a positive and negative difference image threshold in a robust 11.0 - 3.9 micrometer difference image test. This test is the most important cloud determination component in the BCT technique and is used to detect the majority of the clouds in a satellite image. The positive and negative difference image composites derived for each observation time (described below) represent the smallest positive and negative observed difference image values, respectively, for the preceding twenty day period. This test compares the current difference image value to these composite images. A pixel is deemed cloudy if the difference image value is smaller than the negative composite value or if the difference image value, is larger than the positive composite value. The fourth and final test in the BCT cloud detection method involves using the longwave 11.0 micrometer channel information. This infrared threshold test uses a twenty day composite of the second warmest thermal infrared channel values at each pixel location. This product is essentially a "warm" cloud free thermal infrared image. A pixel in the observed infrared image is deemed cloudy if its infrared temperature is colder than the composite infrared threshold value corresponding to its location and time period.

In bispectral composite threshold technique, the 11.0 and 3.9 micrometer channels are used to produce a difference image (11.0-3.9 micrometer) to be used in the generation of the composites. Both positive differences, which mainly occur at low sun angles and at night, and negative differences that occur at all times, are preserved in the difference image. From this difference image information, two composite images are created for each observation time, which represent the smallest negative (values closest to zero) and the smallest positive difference image values, from the preceding twenty day period. The premise here is that difference image values close to zero have the highest probability of representing cloud-free pixels. These composite images serve to provide spatially and temporally varying thresholds for the BCT method. An additional twenty day composite image is also generated for each time using the warmest longwave (11.0 micrometer) brightness

temperature for each pixel from the previous twenty day period. These warm 11.0 micrometer brightness temperature composite images are assumed to represent warm cloud-free thermal images, one for each observation time of day.

The twenty day composite images (positive and negative difference images and the warm 11.0 micrometer images for each hour) used by the BCT algorithm, represent the innovative aspect of the method and provide both spatially and temporally varying clear-sky threshold values for comparison to the observed data. By producing these composites, the BCT approach uses a different threshold value from one pixel to the next and therefore the pixel location, underlying terrain features, present sun angle and other surface conditions (e.g. snow cover) are all implicitly taken into account. These composites capture a large variation in the 11.0 – 3.9 micrometer differences across the region which range from close to zero to above -15 K. The smaller differences (closest to zero) generally occur over water, and the larger values are over land, particularly snow-covered land as in the Rocky Mountains. Rivers can be distinguished from the surrounding land in the composite imagery. The warm infrared brightness temperature composite better represents the thermal structure of the surface than a single threshold value in the absence of clouds. These infrared composite images (from the preceding twenty days) contrast the cold surface of the ocean with warmer land regions during the warm season. The opposite contrast occurs in the cold season. Temperature variations across the domain are considerable (270 - 310 K) and using the composite allows for a spatially representative surface temperature value to be used in the detection approach.

3. Validation of cloud detection techniques

The performance of automated cloud detection algorithms is usually evaluated by comparison to other satellite imagery. However, Schreiner et al. (2001) and Schreiner et al. (1993) used ground based observations from Automated Surface Observing Station (ASOS) and aircraft pilot reports (PIREP) to construct a validation data set. Although limited in coverage and cloud altitude, the use of these data in their evaluation showed that the NESDIS method correctly detected clouds 71% of the time in a 14 month comparison over the continental U.S. region. In a more limited study of a dataset from March 2000, Hawkinson et al. (2001) reported that the method determined the correct sky conditions (cloudy and clear) 75% of the time.

A few studies have used the subjective determination of the presence of clouds to generate a “truth” data set for the quantitative evaluation of the accuracy of a particular scheme. Saunders and Kriebel (1988) determined the presence of a cloud over a region by visually identifying clouds in the satellite imagery for 250 points over a limited region over Europe. They used this data set to validate the performance of their algorithm at in AVHRR data. For a day-time scene from April 14, 1985, the algorithm had a hit rate for cloud detection of 98% but with a false alarm rate of 34% and a skill score of around 65%. These statistics indicate that the application of the algorithm to this data produces a very conservative cloud mask for this AVHRR data set. Merchant et al. (2005) developed a quasi-objective “tailored” mask, using a “widget” in the Interactive Data Language (IDL), which was used as “truth” data to validate their Bayesian approach. Using a 99% clear sky probability as a threshold for a binary mask, they reported a hit rate of 97.2%, and a false alarm rate of 23.7% with a skill score of 73.5 for 43 night-time cases detecting clouds over the western Pacific. This approach

was a significant improvement over the Saunders and Kriebel (1988) method which had a hit rate of 96.3%, a false alarm rate of 32.3% with a skill score of 64.1% for the same data. Jedlovec et al. (2008) took a subjective approach to generating a “truth” data set for validation of the bispectral composite threshold approach to cloud detection with GOES imagery. In their validation work, satellite meteorologists manually determined sky conditions for 30 points per time period, per day, during four different months throughout 2004-2005 using GOES visible and infrared imagery. Subjectively determined sky conditions varied by just a few percent between meteorologists and the individual “truth” values were averaged between the meteorologists for each point. Their combined results for night and day applications of the bispectral composite threshold technique applied to GOES data in 4 different seasons produced a hit rate of 84.5%, with a false alarm rate of only 8.1%, with a skill score of 76.4% for 16,675 validation data points. These combined results indicated good performance of the algorithm with only minimal over determination of clouds in the comprehensive data set.

It is often difficult to inter-compare the performance of various cloud detection techniques because they are often used in different settings. Each cloud detection technique may use different satellite sensors, focus on different geographical regions or even times of the day. To better understand an algorithm’s performance relative to another, the algorithms need to be applied to the same data sets allowing for a direct comparison of the resulting cloud masks. The example below presents such a comparison for August 2004 over the eastern two-thirds of the continental U. S. The two algorithms used were the the NASA EOS science team MODIS cloud mask algorithm and the bispectral composite threshold technique (BCT) adapted for MODIS data (Haines et al. 2005). The MODIS collection 5 cloud algorithm (EOS-5; Frey et al. 2008) is similar to that described above with improvements in performance at night and in polar regions by the inclusion of several additional tests. The MODIS collection 5 data set was obtained from the EOS Data Active Archive Center (DAAC). The application of the BCT technique to MODIS data uses five tests applied to the shortwave and longwave infrared window channels and a similar compositing approach. The algorithms were applied to all Terra MODIS passes over the eastern two-thirds of the United States (both day and night) during this case study period. An example of the cloud masks produced by these algorithms is shown in Figure 4 for a nighttime pass on August 5, 2004. Note that the EOS-5 algorithm assigns confidence levels (i.e., cloudy, possibly cloudy, probably clear and clear) to each pixel in the cloud mask with corresponding grey shades in Figure 4 (from white to dark grey, to light grey to transparent, respectively). An appropriate land type color is assigned to clear regions in both products for display. A qualitative comparison of these cloud mask products to the corresponding infrared window channel image indicates that both cloud masks do quite well in capturing the gross cloud features on this day and time. They both capture the obvious cold clouds observed in the infrared image, but some differences exist in cloud detection for low (warm) clouds over the ocean and land regions.

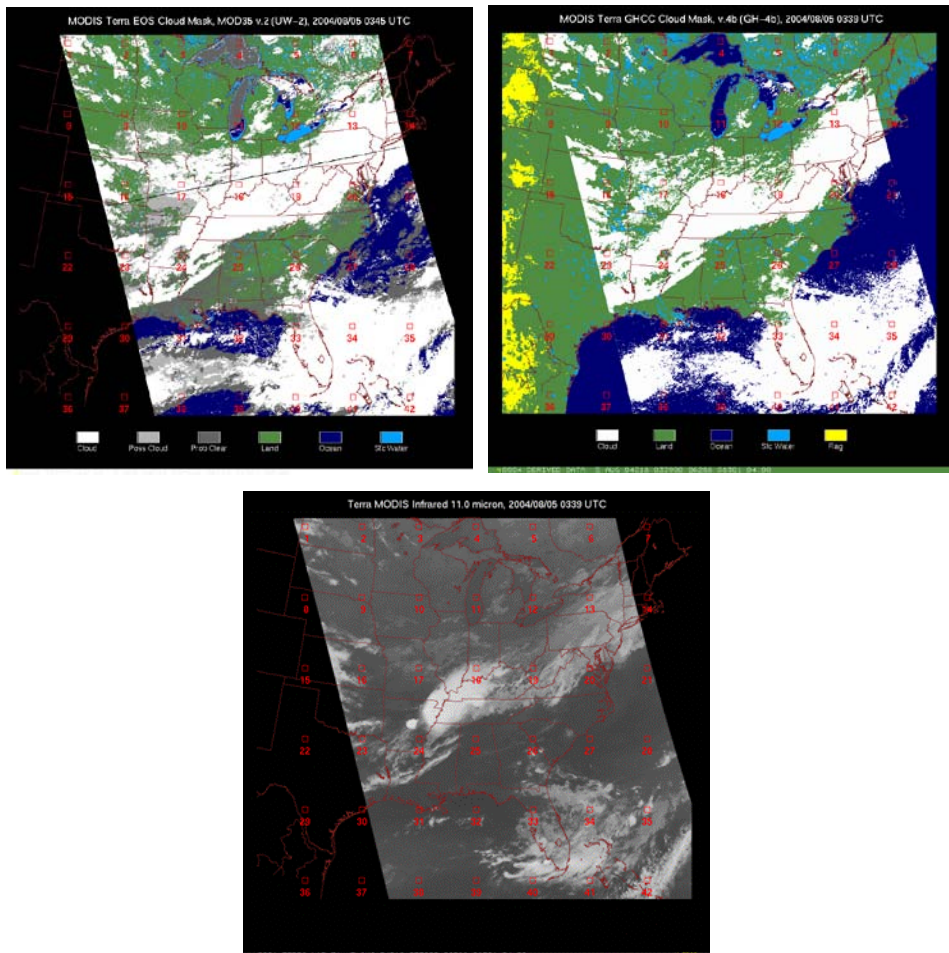


Fig 4. MODIS cloud masks and infrared imagery for August 5, 2004 for the EOS science team collection 5 cloud detection algorithm (upper left) and the bispectral composite threshold technique (upper right). The corresponding infrared MODIS image is presented in the lower panel. Each image is overlaid with grid boxes used in the validation scheme.

To better quantify the performance of these algorithms in detecting clouds over this region, the determination of the presence of clouds by each algorithm was compared to a set of “truth” data subjectively obtained by satellite meteorologists viewing high resolution visible and infrared imagery from MODIS corresponding to the cloud mask times. A fixed set of 42 comparison points were strategically selected over the region as shown on the images in Figure 4. The locations were selected based on a fixed grid with adjustments to include a variety of ocean and land regions (including coastal areas) with a variety of cloud distributions. This validation approach is similar to that used by McNally and Watts (2003) and Alliss et al. (2000)

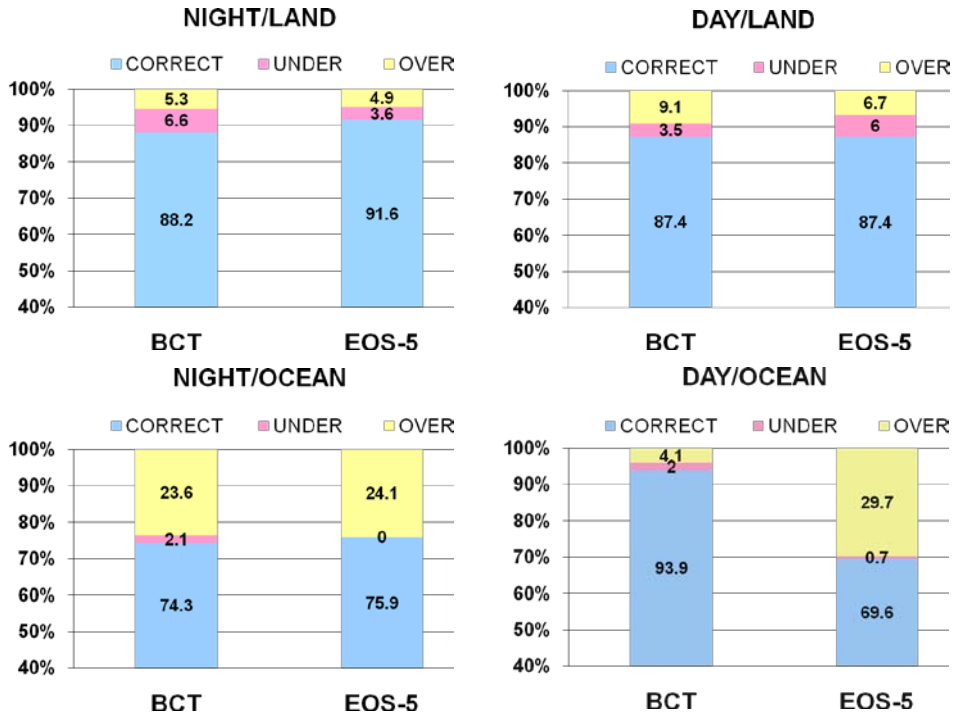


Fig 5. Performance statistics of the bispectral composite threshold (BCT) and the EOS science team collection 5 (EOS-5) MODIS cloud mask algorithm for August 2004 over the eastern half of the United States for night over ocean (upper left), night over land (lower left), day over ocean (upper right), and day over land (lower right). The numbers correspond to the accuracy (%) of the cloud detection algorithm - either correctly determining the correct sky conditions (clear or cloudy - blue bar), or the over- (yellow bar) or under- (pink bar) determination of the cloud conditions.

and nearly identical to that of Jedlovec et al. (2008). For the EOS-5 algorithm, only points having a probability determination of “cloudy” were considered to contain clouds. Other probabilistic determinations (possibly cloudy or probably clear) were considered clear. The statistical results of this comparison were categorized by day and night and land and ocean locations and are presented in Figure 5. Both algorithms perform nearly as well at night, correctly detecting clear or cloudy conditions about 75% of the time over the ocean and around 90% of the time over land. Over the ocean, both schemes over determined the presence of clouds by nearly 25%. Over land, the EOS-5 algorithm correctly determined clear or cloud conditions 91.6 percent of the time, with the remaining misses split between over and under determination. The BCT scheme did nearly as well with 88.2% of the points correct.

The performance of the two algorithms varies significantly during the day over the ocean, with significant over determination of clouds in the EOS-5 scheme contributing to its poor performance. During the day over the ocean, the BCT scheme does extremely well, correctly determining 93.9% of the points. The performance of the two algorithms are similar over

land during the day with 87.4% of the points being determined correctly as being either cloudy or clear. The BCT cloud mask has a slightly greater over determination value than the EOS-5 approach for the points that were incorrectly identified. One should note that the use of only cloud points having the highest confidence were considered cloudy in with the EOS-5 data. If a more conservative cloud choice was used (by including “possibly cloudy” points), the performance statistics for the EOS-5 algorithm would have been worse as a greater number of points would be considered cloudy increasing the over determination of clouds at all times and regions (not shown). This qualitative comparison and statistical analysis indicates that with the proper determination of thresholds, a simple two channel cloud detection technique, such as the bispectral composite threshold approach (Jedlovec et al. 2008), can detect clouds in a variety of situations quite well.

4. Summary

Many different approaches have been used to automatically detect clouds in satellite imagery. Most approaches are deterministic and provide a binary cloud – no cloud product used in a variety of applications. Some of these applications require the identification of cloudy pixels for cloud parameter retrieval, while others require only an ability to mask out clouds for the retrieval of surface or atmospheric parameters in the absence of clouds. A few approaches estimate a probability of the presence of a cloud at each point in an image. These probabilities allow a user to select cloud information based on the tolerance of the application to uncertainty in the estimate. Many automated cloud detection techniques develop sophisticated tests using a combination of visible and infrared channels to determine the presence of clouds in both day and night imagery. Visible channels are quite effective in detecting clouds during the day, as long as test thresholds properly account for variations in surface features and atmospheric scattering. Cloud detection at night is more challenging, since only coarser resolution infrared measurements are available. A few schemes use just two infrared channels for day and night cloud detection. The most influential factor in the success of a particular technique is the determination of the thresholds for each cloud test. The techniques which perform the best usually have thresholds that are varied based on the geographic region, time of year, time of day and solar angle.

5. References

- Ackerman, S. A., et al., (1998). Discriminating clear-sky from clouds with MODIS, *J. Geophys. Res.* Vol. 103, pp. 32,141-32,158.
- Alliss, R. J., et al. (2000). The development of cloud retrieval algorithms applied to GOES digital data, 10th Conference on Satellite Meteorology and Oceanography, Amer. Meteor. Soc., Long Beach, 2000, pp. 330-333.
- Coakley, J. A., and F. P. Bretherton, (1982). Cloud cover from high-resolution scanner data: Detecting and allowing for partially filled fields of view, *J. Geophys. Res.*, Vol. 87, pp. 4917-4932.
- Frey, R. A., S. A. Ackerman, Y. Liu, K. I. Strabala, H. Zhang, J. R. Key, and X. Wang, (2008). Cloud detection with MODIS. Part I. Improvements in the MODIS cloud mask for collection 5. *J. Tech.*, 25, 1057-1072.

- Goodman, A. H., and A. Henderson-Sellers, (1988). Cloud detection and analysis: A review of recent progress, *Atmos. Res.*, Vol. 21, pp. 203-228.
- Haines, S. L., et al., (2005). Spatially Varying Spectral Thresholds for MODIS Cloud Detection, 13th Conference Satellite Meteorology and Oceanography. Amer. Meteor. Soc. Norfolk, [Online] Available http://ams.confex.com/ams/13SATMET/techprogram/paper_79134.htm
- Hawkinson, J. A. et al. (2001). A validation study of the GOES sounder cloud top pressure product, 11th Conference on Satellite Meteorology and Oceanography, Amer. Meteor. Soc., Madison, 2001, pp. 348-350.
- Jedlovec, G. J., S. L. Haines, and F. J. LaFontaine, (2008). Spatial and temporal varying thresholds for cloud detection in GOES imagery. *IEEE Trans. Geosci. Rem. Sens.*, Vol 46, No. 6, 1705-1717.
- King, M. D., et al., (2003). Cloud and aerosol and water vapor properties, precipitable water, and profiles of temperature and humidity from MODIS, *IEEE Trans. Geosci. Remote Sensing*, Vol. 41, pp. 442-458.
- Maturi, E., et al., 2008: NOAA's sea surface temperature products from operational geostationary satellites. *Bull. Amer. Meteor. Soc.*, Vol. 89 pp 1877-1888.
- McNally, A. P., and P. D. Watts, 2003: A cloud detection algorithm for high-spectral-resolution infrared sounders. *Q. J. R. Meteorol. Soc.* Vol. 129, 3411-3423.
- Merchant, C. J., et al., (2005). Probabilistic physically based cloud screening of satellite infrared imagery for operational sea surface temperature retrieval, *Q. J. R. Meteorol. Soc.*, Vol. 31, pp. 2735-2755.
- Reuter, M., et al., 2009: The CM-SAF and FUB Ccloud detection schemes for SEVIRI: Validation with synoptic data and initial comparison with MODIS and Calipso. *J. Appl. Meteor. And Climate*, Vol. 48, pp 301-316.
- Rossow, W. B., and L. C. Garder, (1993). Cloud Detection Using Satellite Measurements of Infrared and Visible Radiances for ISCCP, *J Climate*, Vol. 6, pp. 2341-2369.
- Saunders, R. W., and K. T. Kriebel, 1988: An improved method for detecting clear sky and cloudy radiances from AVHRR data. *Int. J. Remote Sensing*, Vol. 9, pp 123-150.
- Schreiner, A. J., et al., (1993). A comparison of ground and satellite observations of cloud cover, *Bull. Amer. Meteor. Soc.*, Vol. 74, pp. 1851-1862.
- Schreiner, A. J., et al., (2001). Observations and trends of clouds based on GOES sounder data. *J. Geophys. Res.*, Vol. 116, pp. 20349-20363.
- Schreiner, A. J., (2001). Derived cloud products from the GOES-M imager," 11th Conference on Satellite Meteorology and Oceanography, Amer. Meteor. Soc., Madison, pp. 2001, pp. 420-423.
- Simpson, J. J., and J. I. Gobat, (1995) Improved cloud detection in GOES scenes over land, *Remote Sens. of Environ.*, Vol. 52, pp. 36-54.
- Simpson, J. J., and J. I. Gobat, (1995). Improved cloud detection in GOES scenes over the oceans, *Remote Sens. of Environ.*, Vol. 52, pp. 79-94.